# A CARBON NANOFIBER (CNF) BASED 3-D MICROELECTRODE ARRAY FOR IN-VITRO NEURAL PROLIFERATION AND SIGNAL RECORDING

*Sheng-Po Fang, Pit Fee Jao, Eric Franca, Thomas B. DeMarse, Bruce C. Wheeler[#], and Yong-Kyu Yoon**
University of Florida, Florida, USA

## ABSTRACT

Microelectrode arrays (MEAs) are commonly utilized for stimulating and recording extracellular electrical signals including both local field and action potentials in both *in-vitro* and *in-vivo* neural studies. This work demonstrates the feasibility of 3D microelectrode arrays using a novel carbon nanomaterial, electrospun carbon nanofiber (CNF). CNF MEAs impedance is characterized and compared to that of carbon nanotube MEAs and commercial TiN MEAs. An *in-vitro* culture of CNF electrodes are performed using E18 cortical neurons and analyzed for cell interaction. With these electrodes we are able to detect extracellular neural signals including action potentials from single neurons from an array of CNF electrodes embedded within the substrate of an MEA.

## INTRODUCTION

Microelectrode arrays (MEAs) are utilized in various fields such as pharmacological *in-vitro* studies with dissociated neuronal networks, *in-vivo* implanted MEA studies, and fundamental neuroscience research [1-3]. The primary function of MEAs is for stimulating or recording bioelectric signals from neural tissue. Recent efforts have focused on the better integration of electrodes with neural tissue, improvement in electrical characteristics, and optimization for long-term electrode viability.

A variety of sharpened metals and metal alloys have been utilized over the last 50 years to study brain function [4]. Metals such as platinum and tungsten have a long history as neural electrode materials. Other different novel materials like silicon [5], ceramic [6] and flexible polymer [7] have also been investigated. However, the electrical properties of these materials strongly depend on the dimensions of the electrodes. A typical strategy to decrease the electrode impedance is to increase the exposed area, but this in turn leads to a greater, loss of selectivity and potential increase of tissue damage. Additional colloidal metal layers such as platinum black coating to increase surface roughness can successfully increase the surface area but are mechanically fragile and short time degradation still prevails as a primary challenge.

Recent studies have been are now focused on porous conductive materials to lower the impedance while increasing selectivity and sensitivity. It has been shown that the topographical surface of the electrode has strong influence on cell attachment and migration [8]. Three-dimensional (3D) extracellular matrix surface texture at the scale of several nanometers to micrometers has been identified as important determinates of cell adhesion and interaction [9].

Carbon nanotubes (CNT) were identified as a potential candidate with novel nanoporous topography for this application. Through standard photolithography, high conductivity chemical-vapor-deposited CNT forests can be patterned onto microelectrode arrays [10]. These CNT electrodes show good biocompatibility and interface with neural tissue, and improved electrochemical properties [11]. Despite its chemical inertness and biological compatibility, the integration of CNT with typically metallic electrodes is a challenge in the harsh biological environment. Free standing CNT forests are fragile which limits the 3D aspect ratio of the electrode and must be mechanically reinforced with additional materials. The directional morphology and small diameter/porosity of CNT limits effective neural proliferation, motivating development of new nanomaterial technology.

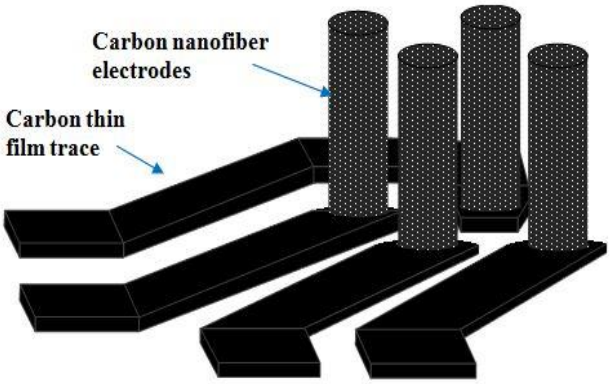


*Figure 1: Schematic of the carbon nanofibrous (CNF) MEAs with conductive carbon film traces.*

Electrospun polymer nanofibers with high surface areas and photolithographical patternability is identified as an alternative. A recent report shows that the polymer nanofiber can be patterned with micrometer resolution and derived into carbon nanofiber (CNF) with a high temperature annealing process resulting in a similar conductivity as CNT [12]. However, photopatterning high aspect ratio microstructures still remains challenging due to the large reflective index mismatch between air and polymer nanofiber. In 2014, an immersion photolithography technique was demonstrated that can enhance the aspect ratio [13]. Moreover, a recent study shows that CNF with high microscale porosity shows improved interactions with cultured neurons than CNT with nanoscale roughness [14].

In this work, the oil immersion lithography process is adopted for high aspect ratio carbon nanofiber microelectrode arrays (CNF MEAs). The design parameters and high temperature carbonization process are optimized to improve the yield rate from 30% to above 95%. Figure 1 shows the schematic of the carbon nanofiber based microelectrode array, where high aspect ratio CNFs make up the electrodes which have high interaction with the neurons. Individual electrical traces were composed of carbon thin film (CTF) connecting each CNF electrodes

with the external recording amplifiers. A living network of spontaneously active E18 rat cortical neurons were cultured on the proposed CNF MEAs. High neural interaction and electro-physiological recording are demonstrated.

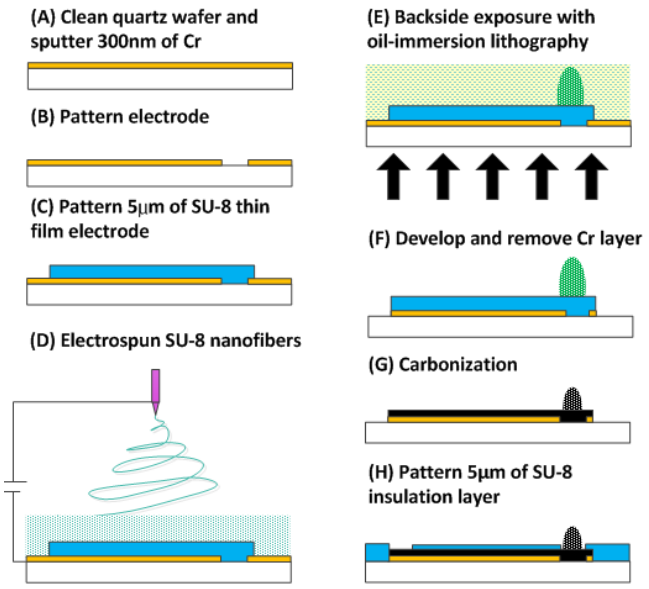


*Figure 2: Fabrication process of the CNF MEAs*

## FABRICATION PROCESS

Quartz is selected as the substrate for CNF MEAs due to its particular benefits including its transparency for use in microscopic studies, backside UV exposure capability, electrical nonconductive property, and non-toxicity for cell culture. Figure 2 shows the fabrication process of CNF MEAs. First, 300 nm chrome is deposited on a quartz substrate by DC sputtering (A). Second, 2 μm of positive resist, Shipley S1818 is spin coated, photolithographically patterned, developed, and chrome is etched to leave 30 μm diameter transparent holes served as the mask for electrodes in a later step (B). Third, SU-8 2005 is spin coated at 3000 rpm to yield a 5 μm thin film and UV patterned as the microelectrode traces and contact pads using a mask aligner (Karl Suss MA6, Suss Inc.) (C). Fourth, SU-8 nanofibers are electrospun using a standard electrospinning setup with an electric field of 1 kV/cm, a distance between the needle tip to collector of 15 cm, and a polymer flow rate of 1 ml/min directly on the patterned quartz substrate (D). Fifth, the SU-8 nanofibers are immersed in an oil index matching medium and exposed to UV light from the backside of the quartz. The 30 μm diameter holes from the first step are used as the electrode mask (E). This immersion lithography greatly enhances patternability of the nanofibers unlike conventional air medium UV exposure yielding poor pattern resolution that limits the aspect ratio for nanofibers due to significant light scattering in the porous medium. This scattering is attributed to similar dimensions of the diameter of the electrospun SU-8 nanofibers ($d_{SU-8}$ = 314.4±7 nm) and the wavelength of the UV light source ($\lambda_{i\text{-}line}$ = 365 nm), and the large optical reflective index mismatch between SU-8 ($n_{SU-8}$ = 1.67) and air ($n_{air}$ = 1). The optical scattering effect has been suppressed by replacing the air medium to an index matching medium with a closer reflective index to that of SU-8. An oil medium with a reflective index of 1.47 is used in this work. After oil immersion lithography, the uncross-linked SU-8 nanofibers are developed and chrome layer is etched to ensure the bottom layer has been electrically insulated (F). High temperature carbonization is performed at 1000$^{O}$C with an optimized ramp rate of 3$^{O}$C/min under the forming gas atmosphere (4% hydrogen and 96% nitrogen) at a flow rate of 13 slm (G). It should be noted that the dimensions of the SU-8 thin film traces and carbonization ramping rates are critical to avoid carbon structure delamination. The MEA yield rate is improved from 30% to over 95% with our optimized process parameters. Finally, a 2 μm SU-8 thin film is spin coated and patterned over the top surface as an electrical insolation layer (H).

## RESULT AND DISCUSSION

Figure 3A shows the optical microscope image of a fabricated CNF MEA. The PDMS reservoir is assembled after the fabrication of the CNF MEA for *in-vitro* cell culture. Scanning electron microscope (SEM) (JEOL 5700) images of the CNF MEA for top view and oblique view are shown in Figure 3B and 3C, respectively. The nanofiber pillar height and diameter were measured from the SEM images. The average height and diameter of the CNF electrode are measured to be 20.7 μm and 23.6 μm, respectively, for 400 mJ/cm$^2$ exposure dosage with 30 μm diameter electrode patterning. CTF traces have an average length of 9.6 mm, a taper width from 230 μm to 80 μm, and a thickness of 2.5 μm after the carbonization process. Approximately 40.8 % vertical size shrinkage and 21.4 % lateral size shrinkage of the SU-8 nanofiber electrodes are observed after carbonization while the overall patterns are preserved.

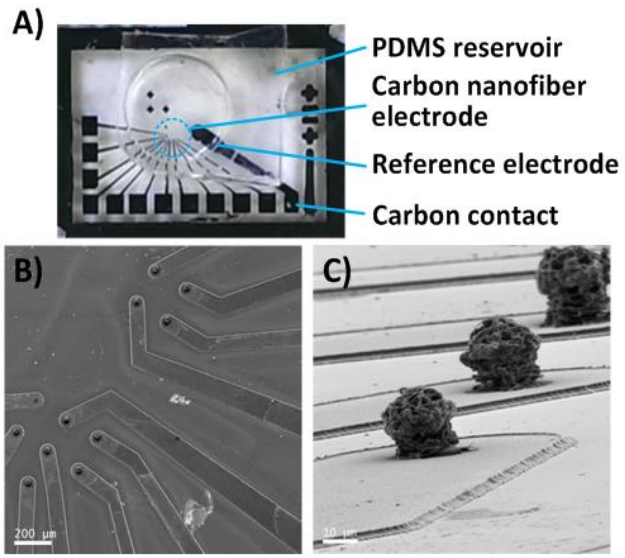


*Figure 3: (A) Photo of a fabricated CNF MEA. SEM images of a MEA: (B) top view and (C) oblique view with CNF electrodes.*

Electrochemical measurements were performed using a two-electrode configuration where the CNF MEA serves as the working electrode. A large Ag/AgCl wire is used as

the reference electrode, and the phosphate-buffered saline (PBS, pH 7) is applied as the electrolyte solution. Electrical characterization of the CNF MEA is performed using an impedance analyzer (4294A, Keysight Inc.). Figure 4 shows the measured impedance with (A) the magnitude and (B) the phase of the fabricated CNF MEA, CNT MEA and commercial stock Titanium Nitride (TiN) MEA (MultiChannel System, Inc.). The basic elements of the experimental setup are: the electrode material resistance, the solution resistance, the charge transfer resistance, and the double layer capacitance. The average measured CNF MEA impedance is 25 kΩ with a phase angle of -16.9° at 1 kHz. At the same frequency, the CNT MEA and commercial stock MEA show an impedance magnitude of 27.6 kΩ and 30.6 kΩ with a phase angle of -35.9° and -72.6°, respectively. The CNF MEA shows lower impedance compared to that of other MEAs at the lower frequency range. Since the CNF MEA shows less double layer capacitance than others, it shows a higher impedance as the frequency increases. Typical neural spike signals have a low frequency of a few kHz and a firing rate of a few times per second [15]. The CNF MEA shows an acceptable impedance around that frequency range compared to other MEAs. The result shows that the CNF can be a good material for future MEAs as it shows very similar electrical properties with other possible benefits such as high cell adhesion, interaction, and sensitivity.

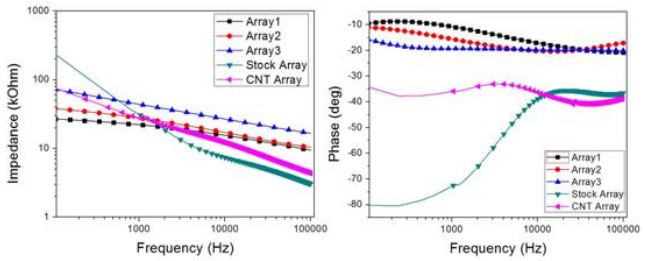


*Figure 4: Impedance measurement of the CNF MEA, CNT MEA, and commercial stock MEA: (A) magnitude and (B) phase.*

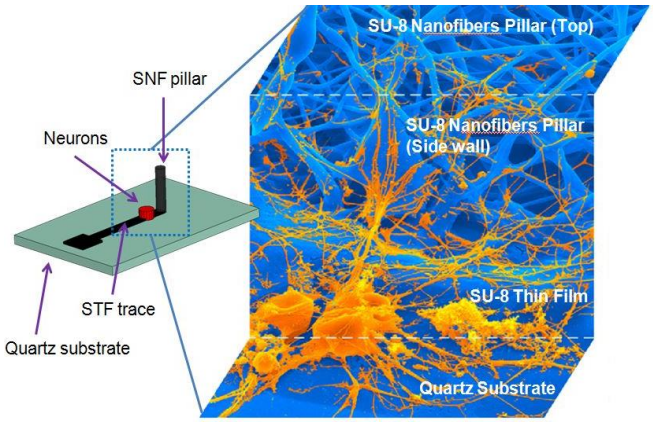


*Figure 5: SEM image of 7 day in-vitro neural growth on a SNF electrode.*

A 7 day *In-vitro* (DIV) analysis on the fabricated CNF MEA was performed using E18 rat cortical neurons from BrainBits LLC, which follows all National Institutes of Health (NIH) guidelines for animal use. The MEAs were treated with plasma for 30 second to increase surface hydrophilicity followed by 0.001 % polyethylenimine (w/v) for supporting long-term cell growth. Cell growth was analyzed via Calcein-AM (Calcein acetoxymethyl ester) staining. In previous study, neurons migrate to the CNF resulting in a higher cell density than the substrate [14]. Figure 5 shows a colored SEM image of neural growth on a fabricated SU-8 nanofiber (SNF) microelectrode after 7 DIV, which illustrates similarity in diameter of the nanofiber and neurons/neurites. High interaction between neurites and the SNF, where neurites grow not only onto but also into the micropores of the SNF, is clearly observed. This interlocking greatly enhances adhesion between nanofibers and neurons/neurites, and may result in enhanced recording signal strengths.

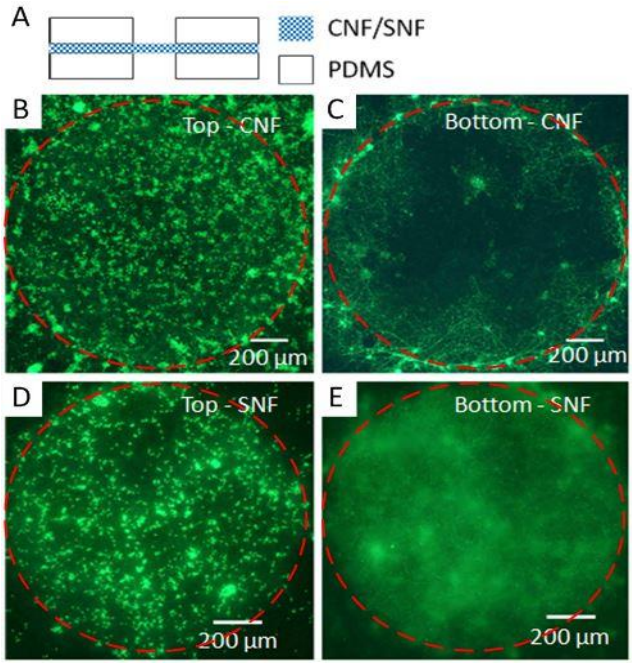


*Figure 6: (A) Schematic of the cross section view of a testing membrane suspended by PDMS: Top and bottom fluorescent images of neural growth on a CNF membrane (B-C), and on a SNF membrane (D-E).*

In order to further understand the neural interaction with carbon/polymer nanofibers, neurons were also cultured for 7 day *in-vitro* on both the CNF and SNF membranes which were suspended between the PDMS structures shown in Figure 6A. The average pore diameter of the CNF and SNF are measured by software ImageJ which were 2.40 µm ± 0.23 µm and 0.87 µm ± 0.07 µm, respectively. Figures 6B and 6D show the fluorescent microscope images of the top sides of the CNF and SNF membranes, respectively, on which neurons were seeded. Lateral growth of neurites and interconnects between neurons were observed. Figure 6C and 6E show the fluorescent microscope images of the bottom sides of the CNF and SNF membranes, respectively. The images reflect that only neurites were capable of growing through these nanoporous membranes. Neuron cell bodies are approximately 10 µm in diameter, which is significantly larger than the pore sizes of both the CNF and SNF

membranes. A higher number of neurites grow through the SNF membrane than the CNF itself as the SNF has a nearly 3 times larger pore size than the CNF allowing neurites to grow through more easily. It also confirms that neurites can grow into the porous CNF electrode which then enhances both neurons adhesion and electrode sensitivity. Moreover, the average neurite length per area on the CNF was measured at 22 mm/mm$^2$, which is 1.5 times longer than one performed under the same experimental condition on the CNT as reported in [14].

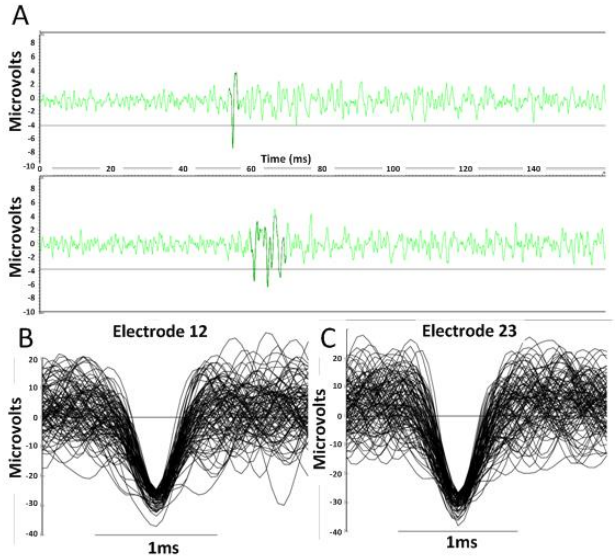


*Figure 7: (A) Examples of extracellular neural signals and putative action potentials (B-C) recorded on two CNF MEA electrodes.*

Evidence of neural activity was obtained using the CNF MEA array after 14 days of culturing in-vitro. Figure 7 provides two examples of the raw electrophysiology from two of the 11 CNF electrodes and example waveforms from putative extracellular action potentials produced by neurons near each electrode. The shape of these neural action potential waveforms recorded by these CNF electrodes typify those commonly reported from commercial planar electrode configurations. Further studies will be necessary to compare the signals recorded from the fabricated CNF electrodes in this study including height and distance to the neural source with signals recorded by the commercially available MEAs. The results show that the CNF electrodes are capable of recording neural signals effectively.

## CONCLUSION

Carbon nanofiber microelectrode arrays were fabricated and optimized to solve the delamination issue due to the thermal stress during carbonization. Reasonable impedance of high aspect ratio CNF MEAs were measured. Cell culture on these MEAs shows high neurite interaction and increased neurite length per area on the 3D CNF electrodes compared with CNT and 2D commercial TiN electrodes. Neurites growth through both the CNF and SNF membrane was also observed. Neural signals including action potentials were successfully recorded on the CNF MEAs. Our results demonstrate the potential CNF MEA electrodes may provide as a promising structure for future studies within the neural sciences and engineering.

## REFERENCES


[1] M. Chiappalone, A. Vato, M. B. Tedesco, M. Marcoli, F. Davide, and S. Martinoia, *Biosensors and Bioelectronics*, vol. 18, pp. 627-634, May. 2003.

[2] A. Stett, U. Egert, E. Guenther, F. Hofmann, T. Meyer, W. Nisch, and H. Haemmerle, *Anal Bioanal Chem.*, 377, pp. 486-495, 2003.

[3] M. Reppel, F. Pollekamp, Z. J. Lu, M. Halbach, K. Brockmeter, B. K. Fleischmann, and J. Hescheler, *Journal of Electrocardiology*, vol. 37, pp. 104-109, 2004.

[4] D. H. Hubel, *Science*, 125, pp. 549-550, 1957.

[5] P. K. Campbell, K. E. Jones, and R. A. Normann, *Biomed. Sci. Instrum.*, vol 26, pp. 161-165, 1990.

[6] K. A. Moxon, S. C. Leiser, G. A. Gerhardt, K. A. Barbee, and J. K. Chapin, *IEEE Trans. Biomed. Eng.*, vol 51, pp. 647–656, 2004.

[7] K. C. Cheung, P. Renaud, H. Tanila, and K. Djupsund, Biosens. Bioelectron, vol 22, pp. 1783–1790, 2007.

[8] C.C. Berry, G. Campbell, A. Spadiccino, M. Robertson, A.S.G. Curtis, *Biomaterials*, vol. 25, pp. 5781-5788, Nov. 2004.

[9] I. Kaverina, O. Krylyshkina, and J.V. Small, *Int. J Biochem Cell Biol*, vol. 7, pp. 746-761, July 2002.

[10] M. P. Mattson, R. C. Haddon, and A. M. Rao, Journal of Molecular Neuroscience, vol. 14, pp. 175-182, June 2000.

[11] K. Wang, H. A. Fishman, H. Dai, and J. S. Harris, *Nano Letter,* vol. 6, no. 9, pp. 2043-2048, 2006.

[12] P.F. Jao, S.-P. Fang, D. E. Senior, K. T. Kim, and Y.K. Yoon, *Electronic Components and Technology Conference (ECTC), 2012 IEEE 62nd,* pp. 2075-2081, 2012.

[13] P.F. Jao, E. Franca, S. P. Fang, B. C. Wheeler, and Y.K. Yoon, *Journal of Microelectromechanical Systems*, vol.24, no.3, pp.703-715, June 2015

[14] E. Franca, P. F. Jao, S. P. Fang, S. Alagapan, L. Pan, J. H. Yoon, Y. K. Yoon, and B. C. Wheeler, *NanoBioscience, IEEE Transactions on*, accepted

[15] T. Yoshida, Y. Masui, R. Eki, A. Iwata, M. Yoshida, and K. Uematsu, *2009 IEEE International Symposium on Circuits and Systems (ISCAS)*, pp.661-664, 24-27 May 2009


## ACKNOWLEDGEMENTS


This work was supported in part by the National Science Foundation (Grant No. 1132413) and the National Institutes of Health (research grant NS 052233).


## CONTACT


[#] B.C. Wheeler, bwheeler@ufl.edu

*Y.K. Yoon, Tel: +1- 352-392-5985; ykyoon@ece.ufl.edu